Molecular Crystals and Liquid Crystals
Publication details, including instructions for authors and subscription information:
http://www.tandfonline.com/loi/gmcl20

On Defects in Biaxial Nematic Films with Random Planar Surface Alignment: A Monte Carlo Study

G. Sai Preeti [a b], C. Chiccoli [c], P. Pasini [c], V. S. S. Sastry [d] & C. Zannoni [a]

[a] Dipartimento di Chimica Industriale "Toso Montanari" and INSTM-CRIMSON, Bologna, Italy

[b] Center for Modeling Simulation and Design, University of Hyderabad, Hyderabad, India

[c] INFN, Sezione di Bologna, Bologna, Italy

[d] School of Physics, University of Hyderabad

Published online: 02 Apr 2013.

To cite this article: G. Sai Preeti, C. Chiccoli, P. Pasini, V. S. S. Sastry & C. Zannoni (2013) On Defects in Biaxial Nematic Films with Random Planar Surface Alignment: A Monte Carlo Study, Molecular Crystals and Liquid Crystals, 573:1, 10-17, DOI: 10.1080/15421406.2012.763214

To link to this article: http://dx.doi.org/10.1080/15421406.2012.763214

Mol. Cryst. Liq. Cryst., Vol. 573: pp. 10–17, 2013

ISSN: 1542-1406 print/1563-5287 online
DOI: 10.1080/15421406.2012.763214

Taylor & Francis
Taylor & Francis Group

On Defects in Biaxial Nematic Films with Random Planar Surface Alignment: A Monte Carlo Study

G. SAI PREETI,[1,2] C. CHICCOLI,[3] P. PASINI,[3] V. S. S. SASTRY,[4] AND C. ZANNONI[1]

[1]Dipartimento di Chimica Industriale "Toso Montanari" and INSTM-CRIMSON, Bologna, Italy
[2]Center for Modeling Simulation and Design, University of Hyderabad, Hyderabad, India
[3]INFN, Sezione di Bologna, Bologna, Italy
[4]School of Physics, University of Hyderabad

We present a detailed computer simulation study of the formation and evolution of topological defects in thin biaxial nematic films. We have used the Straley generalized Hamiltonian and a wide range of biaxial parameters to generate and explore a variety of mesophases. The differences obtained for the various cases are analyzed for thin biaxial nematic films with random planar (Schlieren) surface alignment.

Keywords Computer simulation; Monte Carlo; biaxial nematics; liquid crystals; topological defects

1. Introduction

Topological defects in liquid crystals (LCs) correspond to regions where the director field has some kind of singularity and the scalar order parameter goes to zero. Director singularities are of various dimensionalities, in particular, point ("hedgehogs"), line, and wall defects, and have been extensively studied using theoretical methods and experimental techniques [1–5]. Defects are known to be important in assigning the type of director distribution and indirectly the molecular organization of an LC phase from experimental observations, typically optical textures between crossed polarizers. It is impossible to even just list the huge amount of experimental observations made over the years by a variety of authors on the interpretation of experimental optical textures, but very useful books [6,7] and reviews [4,8] have appeared. Apart from their role in the classification of LC phases, and their importance in studying their phase transitions [9,10], fascinating applications to colloidal systems and their assembly and stability have recently been demonstrated [11]. Theoretical approaches to understanding defects have normally been based on continuum elastic theories [1,2]. However, more recently, spin lattice computer simulations have also been applied to study the involved phenomena [12–17]. In particular, Monte Carlo (MC) studies of defects in uniaxial and biaxial nematic films with different geometries have been performed to simulate the textures that can be experimentally observed using polarizing

*Address correspondence to Paolo Pasini, INFN, Sezione di Bologna, Via Irnerio 46, 40126 Bologna, Italy. E-mail: pasini@bo.infn.it

microscopy [12,13]. The results of the simulations have been validated in various ways and shown to be equivalent, where comparison could be made for these mesoscopic models, to numerical minimization of the elastic free energy for the system subject to appropriate boundary conditions. For instance, it is well known that defects showing both two and four brushes, corresponding to ± 0.5 and ± 1 type topological charges, respectively, are observed in a uniaxial LC phase and this was also shown by MC simulations of uniaxial nematic films [12]. More significantly, MC simulations have proved useful to study complicated systems, such as microdroplets [18], nematic crystals with sprinkled disordering particles [19,20], or defects in nematic shells [21], where analytical solutions would be impractical at best.

One case where the power of the simulation approach can be quite useful [13] is that of biaxial nematic systems [22] where the issue is to what extent textures can be different from those of uniaxial systems, so as to be used for phase assignment, as suggested and experimentally found, at least in some cases, by Chandrasekhar et al. [23] and very recently reconsidered by Picken et al. [24]. The advantage of simulations over the classical free-energy minimization approach based on elastic constants is the sheer number of these (12 for orthorhombic biaxial nematics) and the fact that these constants are essentially unknown. The microscopic approach relies instead only on purely molecular, or rather intermolecular, parameters that are somewhat easier to handle or to guess. Unfortunately, until now, the simulations of defects in biaxial films have been only performed for a model Hamiltonian based on London's approximation of dispersion forces [25]. In that case, it was seen that initially four brush defects appeared, which disappeared by splitting into defects with two brushes [13].

The aim of the present paper is to present a detailed simulation study of biaxial nematic films by using the more general Hamiltonian proposed many years ago by Straley [26] and recently extensively studied by Virga and coworkers [27–29] and by us [30]. This is of value since the detailed study of the phase diagram of this biaxial Hamiltonian has shown a much richer behavior with respect to the simple dispersive one, for instance, with different contiguous phases with respect to the simple dispersive model. It is thus of interest to try to see, as we plan to do in this work, if the differences in the thermodynamics and in the order parameters reflect in the optical textures.

2. The Model System

The microscopic model, as mentioned before, is based on the Hamiltonian proposed by Straley [26] and parametrized by Virga, Romano, and coworkers [27–29]. It is a generalized lattice model, where two parameters (Γ, Λ) define the biaxiality present in the system pair potential U:

$$U = -\varepsilon\{G_{33} - \Gamma\,[G_{11} - G_{22}] + \Lambda\,[2(G_{11} + G_{22}) - G_{33}]\}, \tag{1}$$

where $G_{mn} = P_2({u_m}^i \,.\, {u_n}^j)$, ε denotes a positive constant setting the temperature and the energy scales, $T^* = k_B T/\varepsilon$, P_2 is a Legendre polynomial, and ${u_m}^i$, $m = x, y, z$ represents the axis triplet of molecule i. Here, the biaxial term Γ defines the interaction contribution between the uniaxial and biaxial, and Λ defines that between the biaxial components of the particles. When Γ and Λ vanish, the model reduces to the well-known Lebwhol–Lasher potential [31], which correctly reproduces the uniaxial nematic–isotropic phase transition. A plot of the potential for specific values of Γ and Λ is shown in Fig. 1.

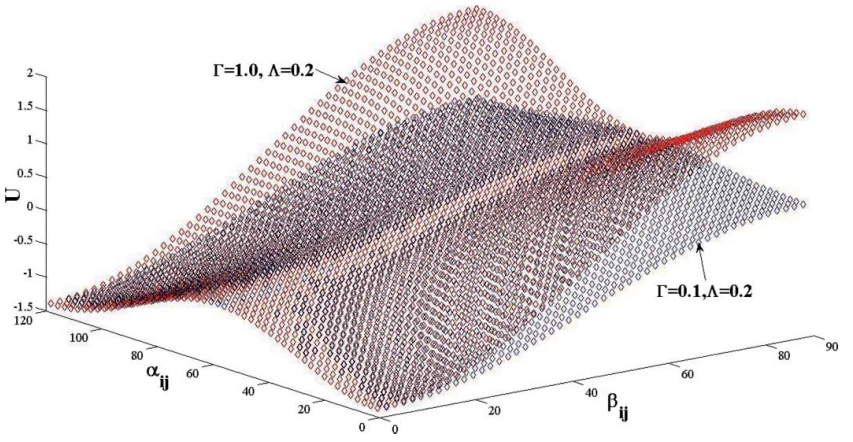

Figure 1. The pair potential for $\Lambda = 0.2$ and $\Gamma = 0.1$ (blue surface) and 1.0 (red surface) as a function of the Euler angles α, β, and keeping γ a constant . The first particle is aligned along the lab axis X, Y, Z, while the second is rotated [35].

The case of London's approximation of dispersion forces, investigated theoretically by Luckhurst–Zannoni–Nordio–Segre [32] and simulated first by Romano and Luckhurst [33] and, more completely, by Biscarini–Chiccoli–Pasini–Semeria–Zannoni [25,34] corresponds to the points in the (Γ, Λ) plane for which $\Lambda = \Gamma^2$.

The phase diagram obtained by MC simulations of the potential in Equation (1) shows the appearance of a biaxial phase at low temperatures for all the values of the parameters Γ and Λ [30]. This biaxial phase could be reached from an isotropic phase either through a uniaxial nematic phase or directly from a biaxial nematic phase, depending on the Γ and Λ values, upon lowering the temperature. An example of phase transitions for a specific value of Γ and Λ in the range (0.0–1.0) is shown in Fig. 2, where the heat capacity versus temperature is reported. In this particular case ($\Gamma = 0.8$), we have no direct biaxial–isotropic transition, but the disordered phase is always reached passing through a uniaxial one [16].

To study the formation of defects in films, we have chosen to simulate samples of size $N = L \times L \times (d + 2)$, where $d << L$ (here $d = 8$) is the thickness of the slab, at a temperature where the bulk system is expected to be deep in a biaxial nematic phase for all Γ and Λ values, i.e., $T^* = k_B T/\varepsilon = 0.1$.

The boundary conditions at the two flat surfaces were chosen as random planar and were implemented by suitable oriented surface layers that were kept frozen during the simulations and modeled by fixing random (x, y) in-plane orientations of the longest molecular axes (director n) and a random alignment of the orthogonal directors l and m. At the other four lateral faces of the system, we left free boundaries, i.e., empty space. The starting configurations of the lattice were chosen to be completely aligned along the lab z-direction (the surface normal) and the evolution of the system was followed according to the classic Metropolis Monte Carlo procedure [36]. Crossed polarizing microscope textures were simulated assuming the spins to act as retarders on the light propagating through the film by means of a Müller matrix approach [37] that we have validated in previous studies. The textures that will be presented here are taken as an average over four Monte Carlo sweeps (MCS).

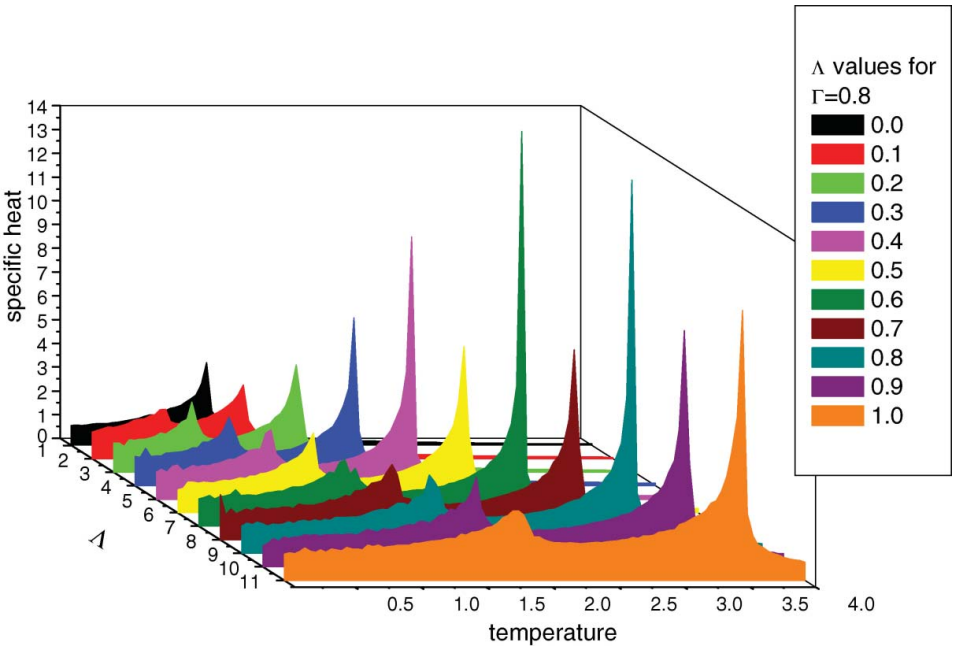

Figure 2. The specific heat profiles for $\Gamma = 0.8$ and different Λ values (0.0–1.0) as a function of temperature.

3. Results and Discussions

As mentioned before, we have investigated biaxial films, of dimensions $120 \times 120 \times (8 + 2)$, with random planar alignment at the surfaces for various choices of the potential parameters (Γ, Λ).

The tangential boundary conditions at the two horizontal surfaces were implemented as described in the previous section. The strength of the interaction at the orienting surfaces was chosen to be the same as that between molecules inside the LC. Typically, the systems were equilibrated over 100,000 MCS and a configuration was stored every 1000 MCS. The film thickness employed was $d = 5.3$ μm and the optical parameters of the biaxial

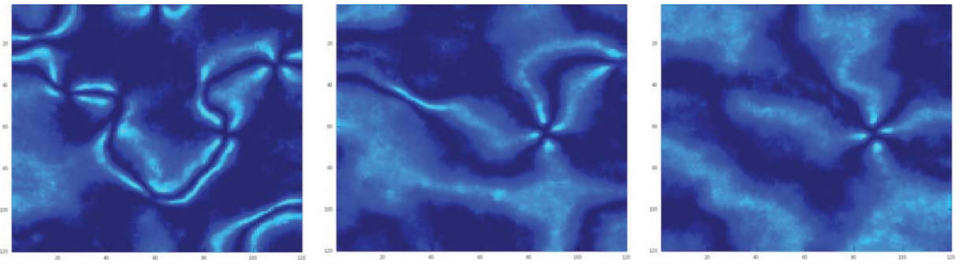

Figure 3. Development of the textures with 17,000 (left), 30,000 (center), and 80,000 (right) MC equilibration sweeps for a random planar geometry system with biaxiality parameters $\Gamma = 0.6$ and $\Lambda = 0.6$.

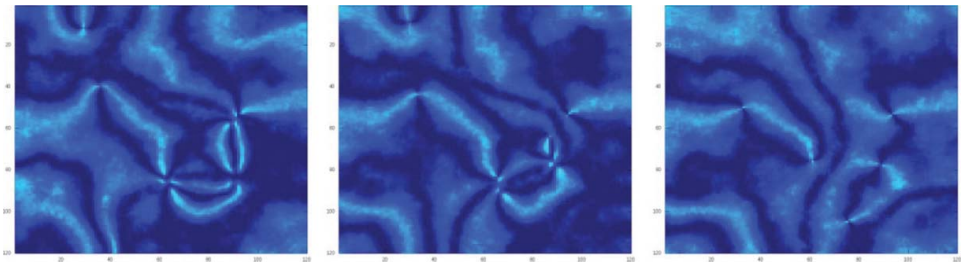

Figure 4. An instance of stabilization of defects of half integral charge at 12,000, 20,000, and 50,000 MCS for the biaxial system with parameters $\Gamma = 0.5$ and $\Lambda = 0.2$.

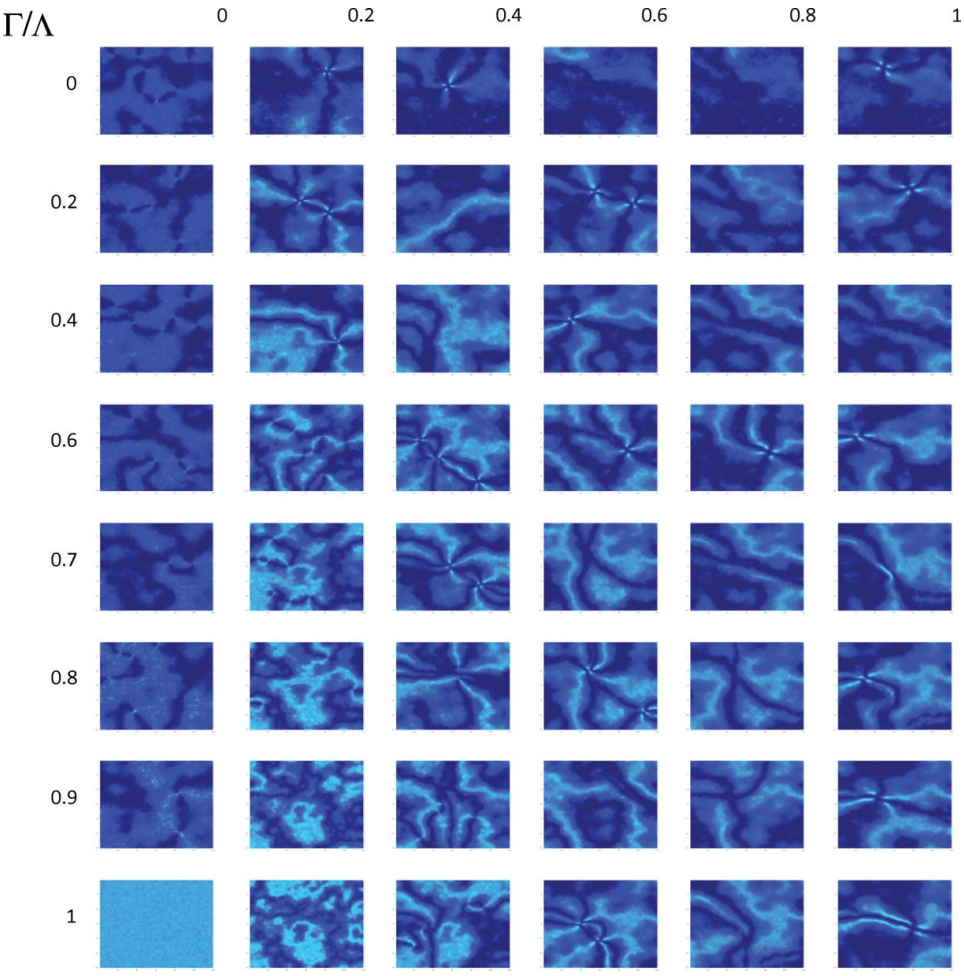

Figure 5. A selection of the textures obtained from MC simulations of a biaxial random planar geometry system for the various values of the parameters (Γ, Λ). The images are taken after 1,000,000 MC cycles.

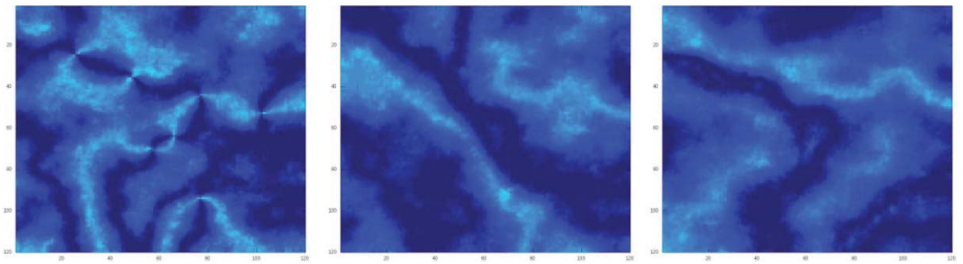

Figure 6. Defects for $\Gamma = 0.6$ and $\Lambda = 0.2$ (left), 0.5 (center), and 0.9 (right) after equilibrating for 75,000 MCS.

nematic were assumed to be: refractive indices $n_x = 1.54$, $n_y = 1.51$, and $n_z = 1.61$ and light wavelength $\lambda_o = 545$ nm.

Examples of the resulting simulated Schlieren textures as observed between crossed polarizers as the system evolves, i.e., at a progressively increasing number of evolution cycles for a system with the biaxial parameters $\Gamma = 0.6$, $\Lambda = 0.6$, and $\Gamma = 0.5$, $\Lambda = 0.2$ are reported in Figs. 3 and 4. The evolutions of defects for the first choice of parameters showed that stable four brushes defects can be formed on equilibration. For the second choice of parameters, the defects of charge ± 1 that were visible initially, split instead into defects of ± 0.5 charge on equilibration, as shown in Fig. 4 for $\Gamma = 0.5$, $\Lambda = 0.2$. These results are in accordance with the previously simulations of a biaxial system based on the dispersion model [13,16]. This kind of splitting of the four brush defects to give stable two brush defects is, however, not visible on further increase of the Λ values.

To perform a systematic investigation, the optical textures after equilibration were computed over the range of Γ [0,1] in steps of 0.1, while Λ was varied from 0 to 1.0 for every value of Γ. A subset of the images obtained for these 100 simulation runs is reported in Fig. 5.

For the set of biaxial constants $\Gamma = 0.6$ and $\Lambda = 0.5$ (Fig. 6, center plate), we observed that the defects that were initially visible disappeared either by collapsing, combining with another one of opposite charge, or due to the simulation constraint. For a system with the biaxial parameters $\Gamma = 0.6$ and $\Lambda = 0.9$ (Fig. 6, right plate), a similar sequence to the above was observed where no stable defects were visible on equilibration.

Over the whole range of the study, it was realized that the lowest values of Λ for every Γ gave rise to stable two brush defects. Varying the values of Γ and Λ produced

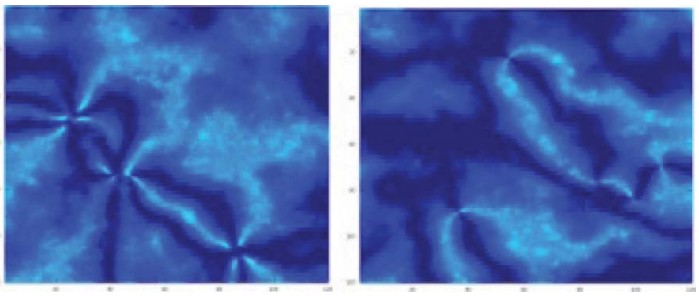

Figure 7. The textures after equilibration for $\Lambda = 0.3$, $\Gamma = 0.6$ (left), and $\Gamma = 0.7$ (right) showing four and two brushes defects, respectively.

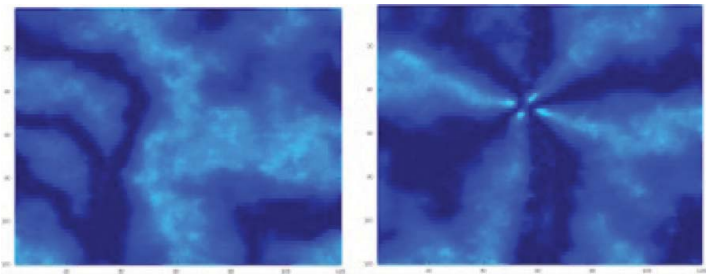

Figure 8. The textures after equilibration for $\Gamma = 0.4$, $\Lambda = 0.4$ (left), and $\Lambda = 0.5$ (right) showing four and two brushes defects, respectively.

considerable changes in the textures, and changes were noted even when a slight change in one of the biaxial parameters was made while keeping the other constant. For instance, $\Gamma = 0.6$ and $\Lambda = 0.3$ gave defects of four brush type (Fig. 7, right plate), but a system with $\Gamma = 0.7$ and $\Lambda = 0.3$ produced stable two brushes defects (Fig. 7, left plate).

A similar observation was made when increasing the Λ value for a particular value of Γ (Fig. 8), even though in some cases, the four brushes defects can annihilate with another of opposite sign or escape from the sample. From these simulations, it seems that only for a region approximately delimited by the relation $\Lambda < \Gamma^2$, the two brushes defects can be produced. This observation is consistent with the previous results obtained by the simulations of the dispersive model (i.e., $\Lambda = \Gamma^2$), which gave a clear indication that the type of defects formed in that case were only of half integral charges, obtained from the splitting of a four-brush defect.

4. Conclusions

We have performed a detailed Monte Carlo study of a $120 \times 120 \times 10$ biaxial nematic film using a generalized Straley lattice Hamiltonian. Various parametrizations of the potential, whose phase transitions and order parameters have been explored in a previous work [30], have been considered and their optical textures have been investigated for Schlieren structures. The defects visible when the biaxial LC film was confined between two surfaces imposing planar degenerate anchoring were either of four or two brushes, depending on the biaxial parameters, and not just two brushes, as observed using the dispersion model [25].

Acknowledgements

This work was supported by the European Union Specific Targeted Research Projects (EU-STREP) Project "Biaxial Nematic Devices" (BIND) FP7-216025. CZ is grateful to the University of Bologna, while CC and PP thank the Istituto Nazionale di Fisica Nucleare (INFN) (grant I.S. BO62) for support.

References

[1] Kleman, M., & Lavrentovich, O. D. (2003). *Soft Matter Physics*. Springer: New York.
[2] Lavrentovich, O. D., Pasini, P., Zannoni, C., & Žumer, S. (eds.). (2001). *Defects in Liquid Crystals: Computer Simulations, Theory and Experiments*. Kluwer: Dordrecht.
[3] Nehring, J., & Saupe, A. (1972). *J. Chem. Soc. Farad. Trans. Ser. II*, *68*, 1

[4] Lavrentovich, O. D., & Pergamenshchik, V. M. (1995). *Int. J. Mod. Phys. B*, *9*, 2389.
[5] Mermin, N. D. (1979). *Rev. Mod. Phys.*, *51*, 647
[6] Demus, D., & Richter, L. (1978). *Textures of Liquid Crystals*. Verlag Chemie: Weinheim.
[7] Dierking, I. (2003). *Textures of Liquid Crystals*. Wiley: New York.
[8] Kleman, M., & Lavrentovich, O. D. (2006). *Phil. Magazine*, *86*, 4117.
[9] Zurek, W. H. (1985). *Nature*, *317*, 505.
[10] Chuang, I, Durrer, R., Turok, N., & Yurke, B. (1991). *Science*, *251*, 1336.
[11] Ravnik, M., Skarabot, M, Zumer, S., Tkalec, U., Poberaj, I., Babic, D., Osterman, N., & Musevic, I., (2007). *Phys. Rev. Lett.*, *99*, 247801.
[12] Chiccoli, C., Lavrentovich, O. D., Pasini, P., & Zannoni, C. (1997), *Phys. Rev. Lett.*, *79*, 4401.
[13] Chiccoli, C., Feruli, I., Lavrentovich, O. D., Pasini, P., Shiyanovskii, S. V., & Zannoni, C. (2002). *Phys. Rev E.*, *66*, 030701.
[14] Billeter, J. L., Smondyrev, A. M., Loriot, G. B., & Pelcovits, R. (2001). In: O. D. Lavrentovich, P. Pasini, C. Zannoni, & S. Zumer (Eds.), *Defects in Liquid Crystals: Computer Simulations, Theory and Experiments*. ch. 6, 141–165. Kluwer: Dordrecht.
[15] Pretzjev, N., & Pelcovits, R. (2002). *Phys. Rev. E*, *66*, 051705.
[16] Chiccoli, C., Pasini, P., Feruli I, & Zannoni, C. (2003). *Mol. Cryst. Liq. Cryst.*, *398*, 195.
[17] Callan-Jones, A. C., Pelcovits, R. A., Slavin, V. A., Zhang, S., Laidlaw, D. H., & Loriot, G. B. (2006). *Phys. Rev. E*, *74*, 06170.
[18] Berggren, E., Zannoni, C., Chiccoli, C., Pasini, P., & Semeria, F. (1994).*Phys. Rev. E*, *49*, 614.
[19] Bellini, T., Buscaglia, M., Chiccoli, C., Mantegazza, F., Pasini, P., & Zannoni, C. (2002). *Phys. Rev. Lett. 88*, 245506.
[20] Rotunno, M., Buscaglia, M., Chiccoli, C., Mantegazza, F., Pasini, P., Bellini, T., & Zannoni, C. (2005). *Phys. Rev. Lett.*, *94*, 097802.
[21] Skacej, G., & Zannoni, C., (2008). *Phys. Rev. Lett.*, *100*, 197802.
[22] Berardi, R., Muccioli, L., Orlandi, S., Ricci, M., & Zannoni, C. (2008). *J. Phys.: Condens. Matter*, *20*, 1.
[23] Chandrashekar, Nair, G. G., Shankar Rao, D. S., Prasad, S. K., Praefcke, K., and Blunk, D. (1998). *Curr. Sci.*, *75*, 1042.
[24] Picken, S. J., Dingemans, T. J., Madsen, L. A., Francescangeli, O., & Samulski, E. T. (2012). *Liq. Cryst.*, *39*, 19.
[25] Biscarini, F., Chiccoli, C., Pasini, P., Semeria, F., & Zannoni, C. (1995). *Phys. Rev. Lett.*, *75*, 1803.
[26] Straley, J. P. (1974), *Phys. Rev. A*, *10*, 1881.
[27] Durand, G. E., Sonnet, A. M., & Virga, E. G. (2003), *Phys. Rev. E*, *67*, 061701.
[28] Romano, S. (2004), *Physica A*, *337*, 505.
[29] Virga, E. G., Romano, S., & DeMatteis, G. (2005). *Phys. Rev. E*, *72*, 041706.
[30] Sai Preeti, G., Murthy, K. P. N., Sastry, V. S. S., Chiccoli, C., Pasini, P, Berardi, R., & Zannoni, C. (2011). *Soft Matter*, *7*, 11483.
[31] Lebwohl, P. A., & Lasher, G. (1972). *Phys. Rev. A*, *6*, 426.
[32] Luckhurst, G. R., Zannoni, C., Nordio, P. L., & Segre, U. (1975). *Mol. Phys.*, *30*, 1345.
[33] Luckhurst, G. R., & Romano, S. (1980). *Mol. Phys.*, *40*, 129.
[34] Chiccoli, C., Pasini, P., Semeria, F., & Zannoni, C. (1999). *Int. J. Mod. Phys. C*, *10*, 469.
[35] Rose, M. E. (1957). *Elementary Theory of Angular Momentum*. Wiley: New York.
[36] Metropolis, N., Rosenbluth, A. W., Rosenbluth, M. N., Teller, A. H., & Teller, E. (1953). *J. Chem. Phys.*, *21*, 1087.
[37] Killian, A. (1993). *Liq. Cryst.*, *14*, 1189.